

Updated analysis of ε'/ε in the standard model with hadronic matrix elements from the chiral quark model

Stefano Bertolini

INFN, Sezione di Trieste and Scuola Internazionale Superiore di Studi Avanzati (SISSA) via Beirut 4, I-34013 Trieste, Italy

Jan O. Eeg

Fysik Institutt, Universitetet i Oslo, N-0316 Oslo, Norway

Marco Fabbrichesi

INFN, Sezione di Trieste and Scuola Internazionale Superiore di Studi Avanzati (SISSA), via Beirut 4, I-34013 Trieste, Italy

(Received 24 February 2000; published 6 February 2001)

We discuss the theoretical and experimental status of the CP violating ratio ε'/ε . We revise our 1997 standard-model estimate—based on hadronic matrix elements computed in the chiral quark model up to $O(p^4)$ in the chiral expansion—by including an improved statistical analysis of the uncertainties and updated determination of the Cabibbo-Kobayashi-Maskawa elements and other short-distance parameters. Using normal distributions for the experimental input data we find $\text{Re } \varepsilon'/\varepsilon = (2.2 \pm 0.8) \times 10^{-3}$, whereas a flat scanning gives $0.9 \times 10^{-3} < \text{Re } \varepsilon'/\varepsilon < 4.8 \times 10^{-3}$. Both results are in agreement with the current experimental data. The key element in our estimate is, as before, the fit of the $\Delta I = 1/2$ rule, which allows us to absorb most of the theoretical uncertainties in the determination of the model-dependent parameters in the hadronic matrix elements. Our semiphenomenological approach leads to numerical stability against variations of the renormalization scale and scheme dependence of the short- and long-distance components. The same dynamical mechanism at work in the selection rule also explains the larger value obtained for ε'/ε with respect to other estimates. A coherent picture of $K \rightarrow \pi\pi$ decays is thus provided.

DOI: 10.1103/PhysRevD.63.056009

PACS number(s): 11.30.Er, 12.39.Fe, 13.25.Es

I. INTRODUCTION

The violation of CP symmetry in the kaon system (for two recent textbooks on the subject see Ref. [1]) is parametrized in terms of the ratios

$$\eta_{00} \equiv \frac{\langle \pi^0 \pi^0 | \mathcal{L}_W | K_L \rangle}{\langle \pi^0 \pi^0 | \mathcal{L}_W | K_S \rangle} \quad \text{and} \quad \eta_{+-} \equiv \frac{\langle \pi^+ \pi^- | \mathcal{L}_W | K_L \rangle}{\langle \pi^+ \pi^- | \mathcal{L}_W | K_S \rangle}. \quad (1.1)$$

Equations (1.1) can be written as

$$\eta_{00} = \varepsilon - \frac{2\varepsilon'}{1 - \omega\sqrt{2}} \approx \varepsilon - 2\varepsilon',$$

$$\eta_{+-} = \varepsilon + \frac{\varepsilon'}{1 + \omega/\sqrt{2}} \approx \varepsilon + \varepsilon', \quad (1.2)$$

where $\omega = A_2/A_0$ is the ratio between the isospin $I=2$ and 0 components of the $K \rightarrow \pi\pi$ amplitudes, the anomalous smallness of which is known as the $\Delta I = 1/2$ selection rule [2]. The complex parameters ε and ε' are introduced to quantify, respectively, indirect (via K_L - K_S mixing) and direct (in the K_L and K_S decays) CP violation. They are measurable quantities, and ε has been known to be nonvanishing since 1964 [3].

The $\Delta S = 1$ effective Lagrangian \mathcal{L}_W is given by

$$\mathcal{L}_W = - \sum_i C_i(\mu) Q_i(\mu), \quad (1.3)$$

where

$$C_i(\mu) = \frac{G_F}{\sqrt{2}} V_{ud} V_{us}^* [z_i(\mu) + \tau y_i(\mu)]. \quad (1.4)$$

In Eq. (1.4), G_F is the Fermi coupling, the functions $z_i(\mu)$ and $y_i(\mu)$ are the Wilson coefficients and V_{ij} the Cabibbo-Kobayashi-Maskawa (CKM) matrix elements; $\tau = -V_{td} V_{ts}^* / V_{ud} V_{us}^*$. According to the standard parametrization of the CKM matrix, in order to determine ε'/ε , we only need to consider the $y_i(\mu)$ components, which control the CP -violating part of the Lagrangian. The coefficients $y_i(\mu)$, and $z_i(\mu)$ contain all the dependence of short-distance physics, and depend on the t, W, b, c masses, the intrinsic QCD scale Λ_{QCD} , the γ_5 -scheme used in the regularization and the renormalization scale μ .

The Q_i in Eq. (1.3) are the effective four-quark operators obtained in the standard model by integrating out the vector bosons and the heavy quarks t, b and c . A convenient and by now standard basis includes the following ten operators:

$$Q_1 = (\bar{s}_\alpha u_\beta)_{V-A} (\bar{u}_\beta d_\alpha)_{V-A},$$

$$Q_2 = (\bar{s}u)_{V-A} (\bar{u}d)_{V-A},$$

$$Q_{3,5} = (\bar{s}d)_{V-A} \sum_q (\bar{q}q)_{V\mp A},$$

$$Q_{4,6} = (\bar{s}_\alpha d_\beta)_{V-A} \sum_q (\bar{q}_\beta q_\alpha)_{V\mp A},$$

$$Q_{7,9} = \frac{3}{2} (\bar{s}d)_{V-A} \sum_q \hat{e}_q (\bar{q}q)_{V\pm A},$$

$$Q_{8,10} = \frac{3}{2} (\bar{s}_\alpha d_\beta)_{V-A} \sum_q \hat{e}_q (\bar{q}_\beta q_\alpha)_{V\pm A}, \quad (1.5)$$

where α, β denote color indices ($\alpha, \beta = 1, \dots, N_c$) and \hat{e}_q are the quark charges ($\hat{e}_u = 2/3$, $\hat{e}_d = \hat{e}_s = -1/3$). Color indices for the color singlet operators are omitted. The labels ($V\pm A$) refer to the Dirac structure $\gamma_\mu(1\pm\gamma_5)$.

The various operators originate from different diagrams of the fundamental theory. At the tree level, we only have the current-current operator Q_2 induced by W -exchange. Switching on QCD, the gluonic correction to tree-level W -exchange induces Q_1 . Furthermore, QCD induces the gluon penguin operators Q_{3-6} . The penguin diagrams induce different operators because of the splitting of the color quark (vector) current into a right- and a left-handed part and the presence of color octet and singlet currents. Electroweak penguin diagrams—where the exchanged gluon is replaced by a photon or a Z -boson and box-like diagrams—induce $Q_{7,9}$ and also a part of Q_3 . The operators $Q_{8,10}$ are induced by the QCD renormalization of the electroweak penguin operators $Q_{7,9}$.

Even though the operators in Eq. (1.5) are not all independent, this basis is of particular interest for any numerical analysis because it has been extensively used for the calculation of the Wilson coefficients to the next-to-leading order (NLO) order in α_s and α_e [4], in different renormalization schemes.

In the standard model, ε' can be in principle different from zero because the 3×3 CKM matrix V_{ij} , which appears in the weak charged currents of the quark mass eigenstate, is in general complex. On the other hand, in other models like the superweak theory [5], the only source of CP violation resides in the K^0 - \bar{K}^0 mixing, and ε' vanishes. It is therefore of great importance for the discussion of the theoretical implications within the standard model and beyond to establish the experimental evidence and precise value of ε' .

The ratio ε'/ε (for a review see, e.g., [6–8]) is computed as

$$\text{Re } \varepsilon'/\varepsilon = e^{i\phi} \frac{G_F \omega}{2|\varepsilon| \text{Re } A_0} \text{Im} \lambda_t \left[\Pi_0 - \frac{1}{\omega} \Pi_2 \right], \quad (1.6)$$

where, the CKM combination $\lambda_t = V_{td} V_{ts}^*$ and, referring to the $\Delta S = 1$ quark Lagrangian of Eq. (1.3),

$$\Pi_0 = \frac{1}{\cos \delta_0} \sum_i y_i \text{Re} \langle Q_i \rangle_0 (1 - \Omega_{\eta+\eta'}), \quad (1.7)$$

$$\Pi_2 = \frac{1}{\cos \delta_2} \sum_i y_i \text{Re} \langle Q_i \rangle_2, \quad (1.8)$$

and $\langle Q_i \rangle_t = \langle 2\pi, I | Q_i | K \rangle$.

We take the phase $\phi = \pi/2 + \delta_0 - \delta_2 - \theta_\varepsilon = (0 \pm 4)^\circ$ as vanishing [9], and we assume everywhere that CPT is conserved. Therefore, $\text{Re } \varepsilon'/\varepsilon = \varepsilon'/\varepsilon$.

Notice the explicit presence of the final-state-interaction (FSI) phases δ_i in Eqs. (1.7) and (1.8). Their presence is a consequence of writing the absolute values of the amplitudes in term of their dispersive parts. Theoretically, given that in Eq. (1.4) $\tau \ll 1$, we obtain

$$\tan \delta_i \approx \frac{\sum_i z_i \text{Im} \langle Q_i \rangle_t}{\sum_i z_i \text{Re} \langle Q_i \rangle_t}. \quad (1.9)$$

Finally, $\Omega_{\eta+\eta'}$ is the isospin breaking (for $m_u \neq m_d$) contribution of the mixing of π with η and η' .

Preliminary remarks

The experiments in the early 1990s [10,11] could not establish the existence of direct CP violation because they agreed only marginally (one of them being consistent with zero [11]) and did not have the required accuracy. During 1999, as we shall briefly recall in the next section, the preliminary analysis of the new run of experiments [12–14] have settled on a range of values consistent with the previous NA31 result, conclusively excluding a vanishing ε' . On the other hand, in order to assess precisely the value we must wait for the completion of the data analysis which will improve the present accuracy by a factor of 2–3.

On the theoretical side, progress has been slow as well because of the intrinsic difficulty of a computation that spans energy scales as different as the pion and the top quark masses. Nevertheless, the estimates available before 1999 [15–17] pointed to a non-vanishing and positive value, with one of them [17] being in the ball park of the present experimental result.

We revise our 1997 estimate [17] of ε'/ε by updating the values of the short-distance input parameters—among which the improved determination of the relevant CKM entries—and by including the Gaussian sampling of the experimental input data. We also update the values and ranges of the “long-distance” model parameters (quark and gluon condensates, and constituent quark mass), by including a larger theoretical “systematic” error ($\pm 30\%$) in the fit of the CP conserving $K \rightarrow \pi\pi$ amplitudes in order to better account for the error related to the truncation of the chiral expansion.

For the sake of comparison with other approaches, we give our results in terms of the so-called B_i -parameters, in two γ_5 regularization schemes: 't Hooft–Veltman (HV) and naive dimensional regularization (NDR).

The combined effect of the new ranges of the input parameters and $\text{Im} \lambda_t$ makes the central value of ε'/ε slightly higher than before, while the statistical analysis of the input parameters reduces the final uncertainty. For a more conservative assessment of the error, we give the full range of uncertainty obtained by the flat span of the allowed ranges of the input parameters. The result is numerically stable as we vary the renormalization scale and scheme. We conclude by

briefly reviewing other estimates of ε' published in the last year.

II. THE EXPERIMENTAL STATUS

Experimentally the ratio ε'/ε is extracted, by collecting K_L and K_S decays into pairs of π^0 and π^\pm , from the relation

$$\left| \frac{\eta_{+-}}{\eta_{00}} \right|^2 \simeq 1 + 6 \operatorname{Re} \frac{\varepsilon'}{\varepsilon}, \quad (2.1)$$

and the determination of the ratios η_{+-} and η_{00} given in Eq. (1.1).

The announcement last year of the preliminary result from the KTeV Collaboration (Fermilab) [12]

$$\operatorname{Re} \varepsilon/\varepsilon' = (2.8 \pm 0.41) \times 10^{-3}, \quad (2.2)$$

based on data collected in 1996-97, and the present result from the NA48 Collaboration (CERN),

$$\operatorname{Re} \varepsilon/\varepsilon' = (1.4 \pm 0.43) \times 10^{-3}, \quad (2.3)$$

based on data collected in 1997 [13] and 1998 [14], settle the long-standing issue of the presence of direct CP violation in kaon decays. However, a clearcut determination of the actual value of ε' at the precision of a few parts in 10^4 must wait for further statistics and scrutiny of the experimental systematics.

By computing the average among the two 1992 experiments (NA31 and E731 [11]) and the KTeV and NA48 data we obtain

$$\operatorname{Re} \varepsilon/\varepsilon' = (1.9 \pm 0.46) \times 10^{-3}, \quad (2.4)$$

where the error has been inflated according to the Particle Data Group procedure ($\sigma \rightarrow \sigma \times \sqrt{\chi^2/3}$), to be used when averaging over experimental data—in our case four sets—with substantially different central values.

The value in Eq. (2.4) can be considered the current experimental result. Such a result will be tested within the next year by the full data analysis from KTeV and NA48 and (hopefully) the first data from KLOE at DAΦNE (Frascati); at that time, the experimental uncertainty will be reduced to a few parts in 10^4 .

The most important outcome of the 1999 results is that direct CP violation has been unambiguously observed and that the superweak scenario, in which $\varepsilon' = 0$, can be excluded to a high degree of confidence (more than 4σ 's).

III. HADRONIC MATRIX ELEMENTS

In the present analysis, we use hadronic matrix elements for all the relevant operators Q_{1-10} and a parameter \hat{B}_K computed in the chiral quark model (χ QM) at $O(p^4)$ in the chiral expansion [17]. This approach has three model-dependent parameters which are fixed by means of a fit of the $\Delta I = 1/2$ rule. Let us here review briefly the model and how the matrix elements are computed.

The χ QM [18] is an effective quark model of QCD which can be derived in the framework of the extended Nambu–

Jona-Lasinio (NJL) model of chiral symmetry breaking (for a review, see, e.g., [19]).

In the χ QM an effective interaction between the u, d, s quarks and the meson octet is introduced via the term

$$\mathcal{L}_{\chi\text{QM}} = -M(\bar{q}_R \Sigma q_L + \bar{q}_L \Sigma^\dagger q_R), \quad (3.1)$$

which is added to an effective low-energy QCD Lagrangian whose dynamical degrees of freedom are the u, d, s quarks propagating in a soft gluon background. The matrix Σ in Eq. (3.1) is the same as that used in chiral perturbation theory and it contains the pseudo-scalar meson multiplet. The quantity M is interpreted as the constituent quark mass in mesons (current quark masses are also included in the effective Lagrangian).

In the factorization approximation, the matrix elements of the four quark operators are written in terms of better known quantities such as quark currents and densities. Such matrix elements (building blocks) like the current matrix elements $\langle 0 | \bar{s} \gamma^\mu (1 - \gamma_5) u | K^+(k) \rangle$ and $\langle \pi^+(p_+) | \bar{s} \gamma^\mu (1 - \gamma_5) d | K^+(k) \rangle$ and the matrix elements of densities, $\langle 0 | \bar{s} \gamma_5 u | K^+(k) \rangle$, $\langle \pi^+(p_+) | \bar{s} d | K^+(k) \rangle$, are evaluated up to $O(p^4)$ within the model. The model dependence in the color singlet current and density matrix elements appears (via the M parameter) beyond the leading order in the momentum expansion, while the leading contributions agree with the well known expressions in terms of the meson decay constants and masses.

Non-factorizable contributions due to soft gluonic corrections are included by using Fierz-transformations and by calculating building block matrix elements involving the color matrix T^a :

$$\langle 0 | \bar{s} \gamma^\mu T^a (1 - \gamma_5) u | K^+(k) \rangle,$$

$$\langle \pi^+(p_+) | \bar{s} \gamma^\mu T^a (1 - \gamma_5) d | K^+(k) \rangle. \quad (3.2)$$

Such matrix elements are non-zero for emission of gluons. In contrast to the color singlet matrix elements above, they are model dependent starting with the leading order. Taking products of two such matrix elements and using the relation

$$g_s^2 G_{\mu\nu}^a G_{\alpha\beta}^a = \frac{\pi^2}{3} \left\langle \frac{\alpha_s}{\pi} GG \right\rangle (\delta_{\mu\alpha} \delta_{\nu\beta} - \delta_{\mu\beta} \delta_{\nu\alpha}) \quad (3.3)$$

makes it possible to express gluonic corrections in terms of the gluonic vacuum condensate [20]. While the factorizable corrections are re-absorbed in the renormalization of the chiral couplings, non-factorizable contributions affect explicitly the form of the matrix elements. The model thus parametrizes all amplitudes in terms of the quantities M , $\langle \bar{q}q \rangle$, and $\langle \alpha_s GG/\pi \rangle$. Higher order gluon condensates are omitted.

The hadronic matrix elements of the operatorial basis in Eq. (1.5) for $K \rightarrow \pi\pi$ decays, have been calculated up to $O(p^4)$ inclusive of chiral loops [17]. The leading order (LO) ($O(p^0, p^2)$) matrix elements $\langle Q_i \rangle_I^{LO}$ and the NLO ($O(p^2, p^4)$) corrections $\langle Q_i \rangle_I^{NLO}$ for final state isospin projections $I=0, 2$ are obtained by properly combining factorizable and non-factorizable contributions and expanding the

result at the given order. The total hadronic matrix elements up to $O(p^4)$ can then be written as

$$\langle Q_i(\mu) \rangle_I = Z_\pi \sqrt{Z_K} [\langle Q_i \rangle_I^{LO} + \langle Q_i \rangle_I^{NLO}] (\mu) + a_i^I(\mu), \quad (3.4)$$

where Q_i are the operators in Eq. (1.5), and $a_i^I(\mu)$ are the contributions from chiral loops (which include the wave-function renormalization). The scale dependence of the $\langle Q_i \rangle_I^{LO, NLO}$ comes from the perturbative running of the quark condensate and masses, the latter appearing explicitly in the NLO corrections. The quantities $a_i^I(\mu)$ represent the scale dependent meson-loop corrections which depend on the chiral quark model via the tree level chiral coefficients. They have been included to $O(p^4)$ in Ref. [17] by applying the modified minimal subtraction ($\overline{\text{MS}}$) scheme in dimensional regularization, as for the χQM calculation of the tree-level chiral coefficients. The wave-function renormalizations Z_K and Z_π arise in the χQM from direct calculation of the $K \rightarrow K$ and $\pi \rightarrow \pi$ propagators.

The hadronic matrix elements are matched—by taking $\mu_{SD} = \mu_{LD}$ —with the NLO Wilson coefficients at the scale $\Lambda_\chi \approx 0.8$ ($\approx m_\rho$) as the best compromise between the range of validity of chiral perturbation and that of strong coupling expansion. The scale dependence of the amplitudes is gauged by varying μ between 0.8 and 1 GeV. In this range the scale dependence of ε'/ε remains always below 10%, thus giving a stable prediction.

A. The fit of the $\Delta I=1/2$ rule

In order to assign the values of the model-dependent parameters M , $\langle \bar{q}q \rangle$ and $\langle \alpha_s GG/\pi \rangle$, we consider the CP -conserving amplitudes in the $\Delta I=1/2$ selection rule of $K \rightarrow \pi\pi$ decays. In practice, we compute the amplitudes

$$A_0 = \frac{G_F}{\sqrt{2}} V_{ud} V_{us}^* \frac{1}{\cos \delta_0} \sum_i z_i(\mu) \text{Re} \langle Q_i(\mu) \rangle_0, \quad (3.5)$$

$$A_2 = \frac{G_F}{\sqrt{2}} V_{ud} V_{us}^* \frac{1}{\cos \delta_2} \sum_i z_i(\mu) \text{Re} \langle Q_i(\mu) \rangle_2 + \omega A_0 \Omega_{\eta+\eta'}, \quad (3.6)$$

within the χQM approach and vary the parameters in order to reproduce their experimental values

$$A_0(K \rightarrow \pi\pi) = 3.3 \times 10^{-7} \text{ GeV}$$

$$\text{and } A_2(K \rightarrow \pi\pi) = 1.5 \times 10^{-8} \text{ GeV}, \quad (3.7)$$

This procedure combines a model for low-energy QCD—which allow us to compute all hadronic matrix elements in terms of a few basic parameters—with the phenomenological determination of such parameters. In this way, some shortcomings of such a naive model (in particular, the matching between long- and short-distance components) are absorbed in the phenomenological fit. As a check, we eventually verify

the stability of the computed observables against renormalization scale and scheme dependence.

The fit of the CP -conserving involves the determination of the final state interaction (FSI) phases. The absorptive component of the hadronic matrix elements appear when chiral loops are included. In our approach the direct determination of the rescattering phases gives at $O(p^4)$ $\delta_0 \approx 20^\circ$ and $\delta_2 \approx -12^\circ$. Although these results show features which are in qualitative agreement with the phases extracted from pion-nucleon scattering [21],

$$\delta_0 = 34.2^\circ \pm 2.2^\circ, \quad \delta_2 = -6.9^\circ \pm 0.2^\circ, \quad (3.8)$$

the deviation from the experimental data is sizable, especially in the $I=0$ component. On the other hand, at $O(p^4)$ the absorptive parts of the amplitudes are determined only at $O(p^2)$ and disagreement with the measured phases should be expected. As a matter of fact, the authors of Ref. [22] find that at $O(p^6)$ the absorptive part of the hadronic matrix elements are substantially modified to give values of the rescattering phases quite close to those in Eq. (3.8). At the same time the $O(p^6)$ corrections to the dispersive part of the hadronic matrix elements are very small.

This result corroborates our ansatz [17] of trusting the dispersive parts of the $O(p^4)$ matrix elements while inputting the experimental values of the rescattering phases in all parts of our analysis, which amounts to taking $\cos \delta_0 \approx 0.8$ and $\cos \delta_2 \approx 1$.

Hadronic matrix elements in the χQM depend on the γ_5 -scheme utilized [17]. Their dependence partially cancels that of the short-distance NLO Wilson coefficients. Because this compensation is only numerical, and not analytical, we take it as part of our phenomenological approach. A formal γ_5 -scheme matching can only come from a model more complete than the χQM . Nevertheless, the result, as shown in Fig. 2 below, is rather convincing.

By taking

$$\Lambda_{\text{QCD}}^{(4)} = 340 \pm 40 \text{ MeV} \quad (3.9)$$

and fitting at the scale $\mu = 0.8$ GeV the amplitudes in Eqs. (3.5) and (3.6) to their experimental values, allowing for a $\pm 30\%$ systematic uncertainty, we find (see Fig. 1)

$$M = 195_{-15}^{+25} \text{ MeV}, \quad \langle \alpha_s GG/\pi \rangle = (330 \pm 5 \text{ MeV})^4,$$

$$\langle \bar{q}q \rangle = (-235 \pm 25 \text{ MeV})^3 \quad (3.10)$$

in the HV scheme, and

$$M = 195_{-10}^{+15} \text{ MeV}, \quad \langle \alpha_s GG/\pi \rangle = (333_{-6}^{+7} \text{ MeV})^4,$$

$$\langle \bar{q}q \rangle = (-245 \pm 15 \text{ MeV})^3 \quad (3.11)$$

in the NDR scheme.

As shown by the light (NDR) and dark (HV) curves in Fig. 2, the γ_5 -scheme dependence is controlled by the value of M , the range of which is fixed thereby. The γ_5 scheme dependence of both amplitudes is minimized for $M \approx 190$ – 200 MeV. The good γ_5 -scheme stability is also

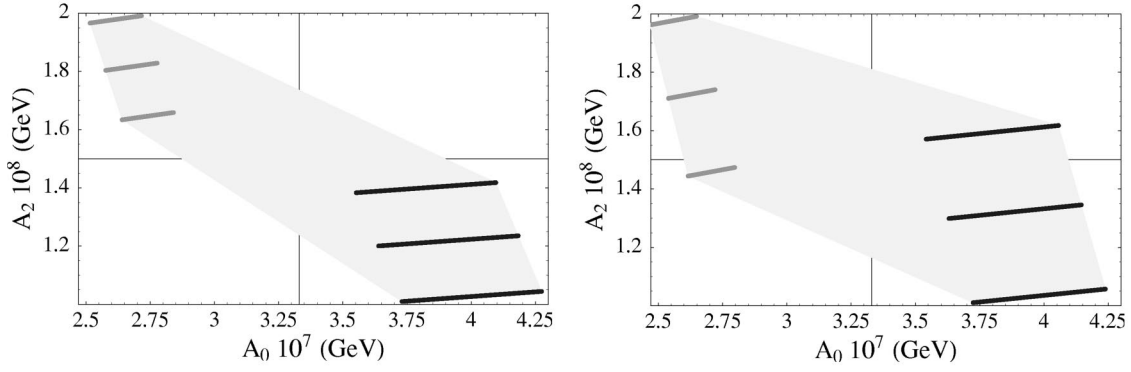


FIG. 1. Dependence of A_0 and A_2 on $\langle \bar{q}q \rangle$, $\langle GG \rangle$, $\Lambda_{\text{QCD}}^{(4)}$ and M at $\mu = 0.8 \text{ GeV}$. The gray and black sets of lines correspond to the extreme values of Λ_{QCD} and M . The length of the lines represents the effect of varying $\langle \bar{q}q \rangle$, while keeping all other parameters fixed. The small dependence of A_2 on the quark condensate is due to the contribution of the electroweak penguins diagrams $Q_{7,8}$. The vertical spread corresponds to varying $\langle \alpha_s GG/\pi \rangle$, with the central line corresponding to the central value of $\langle GG \rangle$. The gray area denotes the region spanned by varying all the parameters without correlations in a $\pm 30\%$ box around the experimental values of A_0 and A_2 given by the cross hairs. The figure on the left (right) shows the HV (NDR) results, corresponding to varying $\langle \bar{q}q \rangle$, $\langle GG \rangle$, $\Lambda_{\text{QCD}}^{(4)}$ and M in the ranges given in Eqs. (3.9)–(3.11).

shown by ε'/ε and \hat{B}_K . For this reason in our previous papers [17] we only quoted for these observables the HV results.

The fit of the amplitude A_0 and A_2 is obtained for values of the quark and gluon condensates which are in agreement with those found in other approaches, i.e., QCD sum rules and lattice, although it is fair to say that the relation between the gluon condensate of QCD sum rules and lattice and that of the χQM is far from obvious. The value of the constituent quark mass M is in good agreement with that found by fitting radiative kaon decays [23].

In Fig. 3 we present the anatomy of the relevant operator contributions to the CP conserving amplitudes. It is worth noticing that, because of the NLO enhancement of the $I=0$ matrix elements (mainly due to the chiral loops), the gluon

penguin contribution to A_0 amounts to about 20% of the amplitude.

Turning now to the $\Delta S=2$ Lagrangian,

$$\mathcal{L}_{\Delta S=2} = -C_{2S}(\mu) Q_{S2}(\mu), \quad (3.12)$$

where

$$C_{2S}(\mu) = \frac{G_F^2 m_W^2}{4\pi^2} [\lambda_c^2 \eta_1 S(x_c) + \lambda_t^2 \eta_2 S(x_t) + 2\lambda_c \lambda_t \eta_3 S(x_c, x_t)] b(\mu) \quad (3.13)$$

where $\lambda_j = V_{jd} V_{js}^*$, $x_i = m_i^2/m_W^2$. We denote by Q_{S2} the $\Delta S=2$ local four quark operator

$$Q_{S2} = (\bar{s}_L \gamma^\mu d_L)(\bar{s}_L \gamma_\mu d_L), \quad (3.14)$$

which is the only local operator of dimension six in the standard model.

The integration of the electroweak loops leads to the Inami-Lim functions [24] $S(x)$ and $S(x_c, x_t)$, the exact expressions of which can be found in the reference quoted, which depend on the masses of the charm and top quarks and describe the $\Delta S=2$ transition amplitude in the absence of strong interactions.

The short-distance QCD corrections are encoded in the coefficients η_1 , η_2 and η_3 with a common scale- and renormalization-scheme-dependent factor $b(\mu)$ factorized out. They are functions of the heavy quarks masses and of the scale parameter Λ_{QCD} . These QCD corrections are available at the NLO [34] in the strong and electromagnetic couplings.

The scale-dependent factor of the short-distance corrections is given by

$$b(\mu) = [\alpha_s(\mu)]^{-2/9} \left(1 - J_3 \frac{\alpha_s(\mu)}{4\pi} \right), \quad (3.15)$$

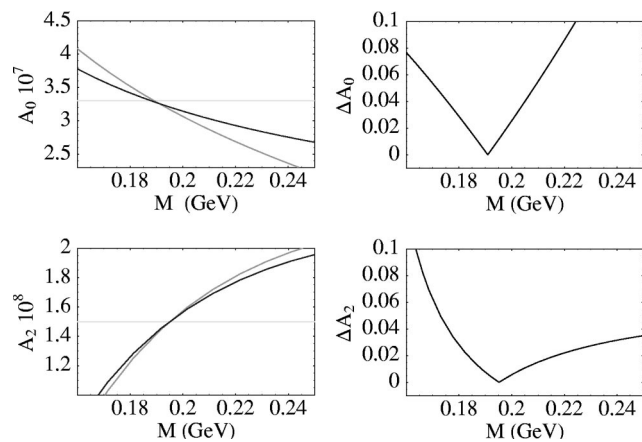


FIG. 2. Test of the γ_5 -scheme stability of the A_0 and A_2 amplitudes as functions of M . The light (dark) curves correspond to the NDR (HV) results, while the horizontal lines mark the experimental values. The two figures on the right plot $\Delta A_i \equiv 2|(A_i^{\text{HV}} - A_i^{\text{NDR}})/(A_i^{\text{HV}} + A_i^{\text{NDR}})|$. For the values of $\langle \bar{q}q \rangle$ and $\langle \alpha_s GG/\pi \rangle$ in Eqs. (3.10), (3.11) we find γ_5 -scheme independence for $M \approx 190\text{--}200 \text{ MeV}$.

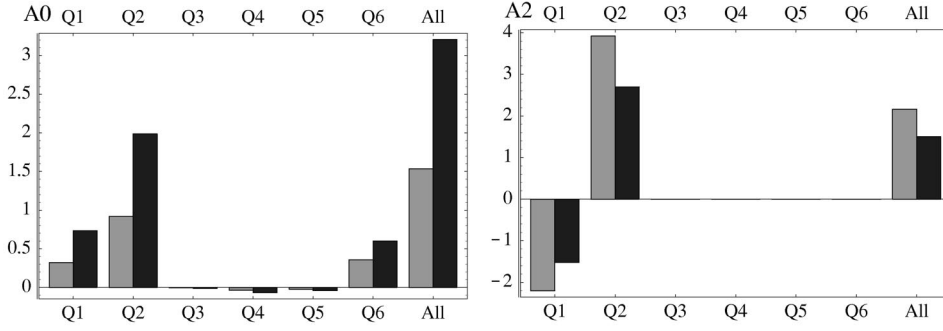


FIG. 3. Operator-by-operator contributions to $A_0 \times 10^7$ and $A_2 \times 10^8$ (GeV) in the HV scheme. In (light) dark is the (LO) NLO value. Notice the $O(p^4)$ enhancement of the gluon penguin operator in the $I=0$ amplitude.

where J_3 depends on the γ_5 -scheme used in the regularization. The NDR and HV scheme yield, respectively,

$$J_3^{\text{NDR}} = -\frac{307}{162} \quad \text{and} \quad J_3^{\text{HV}} = -\frac{91}{162}. \quad (3.16)$$

On the long-distance side, the hadronic B_K parameter is introduced by writing the $\Delta S=2$ matrix element as

$$\langle \bar{K}^0 | Q_{S2}(\mu) | K^0 \rangle = \frac{4}{3} f_K^2 m_K^2 B_K(\mu). \quad (3.17)$$

The scale- and renormalization-scheme- independent parameter \hat{B}_K is then defined by means of Eqs. (3.15)–(3.17) as

$$\hat{B}_K = b(\mu) B_K(\mu). \quad (3.18)$$

By using the input values found by fitting the $\Delta I=1/2$ rule we obtain in both γ_5 schemes

$$\hat{B}_K = 1.1 \pm 0.2. \quad (3.19)$$

The result (3.19) includes chiral corrections up to $O(p^4)$ and it agrees with what we found in [17]. In the chiral limit one derives a simple expression for \hat{B}_K [Eq. (6.3) in Ref. [17]], which depends crucially on the value of the gluon condensate. In this limit, for central values of the parameters, we obtain $\hat{B}_K = 0.44$ (0.46) in the HV (NDR) scheme. A recent calculation of \hat{B}_K , based on QCD sum rules, finds in the chiral limit and to the NLO in the $1/N$ expansion $\hat{B}_K = 0.41 \pm 0.09$ [25]. Many calculations of B_K have been performed on the lattice (for a recent review see [26]). According to Ref. [26], the analysis of Ref. [27] presents the most extensive study of systematic errors and gives the (quenched) value $\hat{B}_K = 0.86 \pm 0.06 \pm 0.14$, which should be taken as the present reference value, while awaiting for further progress in including dynamical quarks on the lattice.

Notice that no estimate of ε'/ε can be considered complete unless it also gives a value for \hat{B}_K . The case of the χ QM, for instance, is telling insofar as the enhancement of B_6 is partially compensated for by a large \hat{B}_K (and accordingly a smaller $\text{Im} \lambda_t$).

B. The factors B_i

The factors B_i , defined as

$$B_i \equiv \langle Q_i \rangle^{\text{model}} / \langle Q_i \rangle^{\text{VSA}} \quad (3.20)$$

have become a standard way of displaying the values of the hadronic matrix elements in order to compare them among various approaches. However they must be used with care because of their dependence on the renormalization scheme and scale, as well as on the choice of the vacuum saturation approximation (VSA) parameters.

They are given in the χ QM in Table I in the HV and NDR schemes, at $\mu = 0.8$ GeV, for the central value of $\Lambda_{\text{QCD}}^{(4)}$. The dependence on Λ_{QCD} enters indirectly via the fit of the $\Delta I = 1/2$ selection rule and the determination of the parameters of the model.

The uncertainty in the matrix elements of the penguin operators Q_{5-8} arises from the variation of $\langle \bar{q}q \rangle$. This affects mostly the $B_{5,6}$ parameters because of the leading linear dependence on $\langle \bar{q}q \rangle$ of the $Q_{5,6}$ matrix elements in the χ QM, contrasted to the quadratic dependence of the corresponding VSA matrix elements. Accordingly, $B_{5,6}$ scale as $\langle \bar{q}q \rangle^{-1}$, or via PCAC as m_q , and therefore are sensitive to the value

TABLE I. Central values of the B_i factors in the HV and NDR renormalization schemes. For $B_{5,6}$ the leading scaling dependence on $\langle \bar{q}q \rangle$ is explicitly shown for a conventional value of the condensate. All other B_i factors are either independent or very weakly dependent on $\langle \bar{q}q \rangle$. The dependence on $\langle \alpha_s GG/\pi \rangle$ in the ranges of Eqs. (3.10), (3.11) remains always below 10%.

	HV	NDR
$B_1^{(0)}$	9.3	9.7
$B_2^{(0)}$	2.8	2.9
$B_1^{(2)} = B_2^{(2)}$	0.42	0.39
B_3	-2.3	-3.0
B_4	1.9	1.3
$B_5 \simeq B_6$	$1.8 \times \frac{(-240 \text{ MeV})^3}{\langle \bar{q}q \rangle}$	$1.3 \times \frac{(-240 \text{ MeV})^3}{\langle \bar{q}q \rangle}$
$B_7^{(0)} \simeq B_8^{(0)}$	2.6	2.4
$B_9^{(0)}$	3.5	3.4
$B_{10}^{(0)}$	4.3	5.2
$B_7^{(2)} \simeq B_8^{(2)}$	0.89	0.84
$B_9^{(2)} = B_{10}^{(2)}$	0.42	0.39

chosen for these parameters. For this reason, we have reported the corresponding values of $B_{5,6}$ when the quark condensate in the VSA is fixed to its PCAC (partial conservation of axial-vector coupling) value.

It should however be stressed that such a dependence is not physical and is introduced by the arbitrary normalization on the VSA result. The estimate of ε' is therefore almost independent of m_q , which only enters the NLO corrections and the determination of \hat{B}_K .

The enhancement of the $Q_{5,6}$ matrix elements with respect to the VSA values [the conventional normalization of the VSA matrix elements corresponds to taking $\langle \bar{q}q \rangle (0.8 \text{ GeV}) \simeq (-220 \text{ MeV})^3$] is mainly due to the NLO chiral loop contributions. Such an enhancement, due to final state interactions, has been found in $1/N_c$ analyses beyond LO [28,29], as well as recent dispersive studies [30,32]. A large- N_c approach, based on QCD sum rules [33] which reproduces the electroweak $\pi^+ - \pi^-$ mass difference and the leptonic $\pi(\eta)$ rare decays, disagrees in the determination of $\langle Q_7 \rangle_{0,2}$ at $\mu = 0.8 \text{ GeV}$, due to the sharp scale dependence found for these matrix elements. Since the operator Q_7 gives a negligible contribution to ε'/ε , we should wait for a calculation of other matrix elements within the same framework in order to assess the extent and the impact of the disagreement with the χ QM results.

Among the non-factorizable corrections, the gluon condensate contributions are most important for the CP -conserving $I=2$ amplitudes (and account for the values and uncertainties of $B_{1,2}^{(2)}$) but are otherwise inessential in the determination of ε' , for which FSI are the most relevant corrections to the LO $1/N$ result.

IV. BOUNDS ON $\text{Im } \lambda_T$

The updated measurements for the CKM elements $|V_{ub}/V_{cb}|$ implies a change in the determination of the Wolfenstein parameter η that enter in $\text{Im } \lambda_i$. This is of particular relevance because it affects proportionally the value of ε'/ε .

The allowed values for $\text{Im } \lambda_i \simeq \eta |V_{us}| |V_{cb}|^2$ are found by imposing the experimental constraints for ε , $|V_{ub}/V_{cb}|$, Δm_d and Δm_s which give rise to the following equations:

$$\begin{aligned} & \eta \left(1 - \frac{\lambda^2}{2}\right) \left\{ \left[1 - \rho \left(1 - \frac{\lambda^2}{2}\right)\right] |V_{cb}|^2 \eta_2 S(x_t) \right. \\ & \left. + \eta_3 S(x_x, x_t) - \eta_1 S(x_c) \right\} \frac{|V_{cb}|^2}{\lambda^8} \hat{B}_K = \frac{|\varepsilon|}{C \lambda^{10}}, \end{aligned} \quad (4.1)$$

where

$$C = \frac{G_F^2 f_K^2 m_K^2 m_W^2}{3\sqrt{2}\pi^2 \Delta M_{LS}} \quad \text{and} \quad x_i = m_i^2/m_W^2, \quad (4.2)$$

and

$$\eta^2 + \rho^2 = \frac{1}{\lambda^2} \frac{|V_{ub}|^2}{|V_{cb}|^2}, \quad (4.3)$$

$$\eta^2 \left(1 - \frac{\lambda^2}{2}\right)^2 + \left[1 - \rho \left(1 - \frac{\lambda^2}{2}\right)\right]^2 = \frac{1}{\lambda^2} \frac{|V_{td}|^2}{|V_{cb}|^2}, \quad (4.4)$$

where $|V_{td}|$ is found by means of

$$\Delta m_d = \frac{G_F}{24\sqrt{2}\pi^2} |V_{td}|^2 |V_{tb}|^2 m_{B_d} f_{B_d}^2 B_{B_d} \eta_B x_t F(x_t) \quad (4.5)$$

and

$$\frac{\Delta m_s}{\Delta m_d} = \frac{m_{B_s} f_{B_s}^2 B_{B_s} |V_{ts}|^2}{m_{B_d} f_{B_d}^2 B_{B_d} |V_{td}|^2}. \quad (4.6)$$

The functions $F(x)$ in Eq. (4.5) and $S(x)$ in Eq. (4.1) can be found in [24].

By using the method of Parodi, Roudeau and Stocchi [35], who have run their program starting from the inputs listed in Table II and

$$\eta_1 = 1.44 \pm 0.18, \quad \eta_2 = 0.52, \quad \eta_3 = 0.45 \pm 0.01, \quad (4.7)$$

which are the values we find for our inputs, it is found that

$$\text{Im } \lambda_t = (1.14 \pm 0.11) \times 10^{-4}, \quad (4.8)$$

where the error is determined by the Gaussian distribution in Fig. 4. Notice that the value thus found is roughly 10% smaller than those found in other estimates for which \hat{B}_K is smaller.

The effect of this updated fit is a substantial reduction in the range of $\text{Im } \lambda_t$ with respect to what we used in our 1997 estimate [17]: all values smaller than 1.0×10^{-4} are now excluded (as opposed as before when values as small as 0.6×10^{-4} were included).

V. ESTIMATING ε'/ε

The value of ε' computed by taking all input parameters at their central values (Table II) is shown in Fig. 5. The figure shows the contribution to ε' of the various operators in two γ_5 renormalization schemes at $\mu = 0.8 \text{ GeV}$ and 1.0 GeV . The advantage of such a histogram is that, contrary to the B_i , the size of the individual contributions does not depend on some conventional normalization.

As the histogram makes it clear, the two dominant contributions come from the gluon and electroweak penguin operators, Q_6 and Q_8 . However, the gluon penguin operator dominates and there is very little cancellation with the electroweak penguin operator. The dominance of the $I=0$ components in the χ QM originates from the $O(p^4)$ chiral corrections, the detailed size of which is determined by the fit of the $\Delta I=1/2$ rule. It is a nice feature of the approach that the renormalization scheme stability imposed on the CP conserving amplitudes is numerically preserved in ε'/ε . The comparison of the two figures shows also the remarkable

TABLE II. Numerical values of the input parameters used in the present analysis. The triangles mark those that have been updated with respect to our 1997 estimate.

	Parameter	Value
	V_{ud}	0.9753
	V_{us}	0.2205 ± 0.0018
	$\sin^2 \theta_W$	0.2247
	m_Z	91.187 GeV
	m_W	80.22 GeV
	$\bar{m}_b(m_b)$	4.4 GeV
▷	$\bar{m}_c(m_c)$	1.3 GeV
▷	$ \varepsilon $	$(2.280 \pm 0.019) \times 10^{-3}$
▷	$ V_{cb} $	0.0405 ± 0.0015
▷	$ V_{ub}/V_{cb} $	0.080 ± 0.017 (CLEO), 0.104 ± 0.019 (LEP)
▷	$\bar{m}_t(m_t)$	165 ± 5 GeV
	\hat{B}_K	1.1 ± 0.2
▷	Δm_s	> 12.4 ps $^{-1}$
▷	Δm_d	(0.472 ± 0.016) ps $^{-1}$
▷	$f_{B_d} \sqrt{B_{B_d}}$	(210_{-32}^{+39}) MeV
▷	$\xi \equiv f_{B_s} \sqrt{B_{B_s}} / f_{B_d} \sqrt{B_{B_d}}$	$1.11_{-0.04}^{+0.06}$
▷	$m_{B_d^0}$	5.2792 ± 0.0018 GeV
▷	$m_{B_s^0}$	5.3693 ± 0.0020 GeV
▷	η_B	0.55 ± 0.01
	$f_\pi = f_{\pi^+}$	92.4 MeV
	$f_K = f_{K^+}$	113 MeV
	$m_\pi = (m_{\pi^+} + m_{\pi^0})/2$	138 MeV
	$m_K = m_{K^0}$	498 MeV
	m_η	548 MeV
	Λ_χ	$2\sqrt{2} \pi f_\pi$
▷	$\Omega_{\eta+\eta'}$	0.25 ± 0.10
	$\Lambda_{\text{QCD}}^{(4)}$	340 ± 40 MeV
	$\bar{m}_u + \bar{m}_d$ (1 GeV)	12 ± 2.5 MeV
▷	\bar{m}_s (1 GeV)	150 ± 25 MeV
▷	$\langle \bar{q}q \rangle$	HV: $(-235 \pm 25 \text{ MeV})^3$, NDR: $(-245 \pm 15 \text{ MeV})^3$
▷	$\langle \alpha_s GG/\pi \rangle$	HV: $(330 \pm 5 \text{ MeV})^4$, NDR: $(333_{-6}^{+7} \text{ MeV})^4$
▷	M	HV: $195_{-15}^{+25} \text{ MeV}$, NDR: $195_{-10}^{+15} \text{ MeV}$

renormalization scale stability of the central value once the perturbative running of the quark masses and the quark condensate is taken into account.

In what follows, the model-dependent parameters M , $\langle \alpha_s GG/\pi \rangle$ and $\langle \bar{q}q \rangle$ are uniformly varied in their given ranges (flat scanning), while the others are sampled according to their normal distributions (see Table II for the ranges used). Values of ε'/ε found in the HV and NDR schemes are included with equal weight.

For a given set, a distribution is obtained by collecting the values of ε'/ε in bins of a given range. This is shown in Fig. 6 for a particular choice of bins. The final distribution is partially skewed, with more values closer to the lower end but a longer tail toward larger values. However, because the skewness of the distribution is less than one, the mean and the standard deviation are a good estimate of the central

value and the dispersion of values around it. This statistical analysis yields

$$\varepsilon'/\varepsilon = (2.2 \pm 0.8) \times 10^{-3}. \quad (5.1)$$

A more conservative estimate of the uncertainties is obtained via the flat scanning of the input parameters, which gives

$$0.9 \times 10^{-3} < \text{Re } \varepsilon'/\varepsilon < 4.8 \times 10^{-3}. \quad (5.2)$$

In both estimates a theoretical systematic error of $\pm 30\%$ is included in the fit of the CP conserving amplitudes A_0 and A_2 .

The stability of the numerical outcomes is only marginally affected by shifts in the value of $\Omega_{\eta+\eta'}$ due to NLO chiral corrections [36] and by additional isospin breaking effects [37–39]. Any effective variation of $\Omega_{\eta+\eta'}$ is anti-

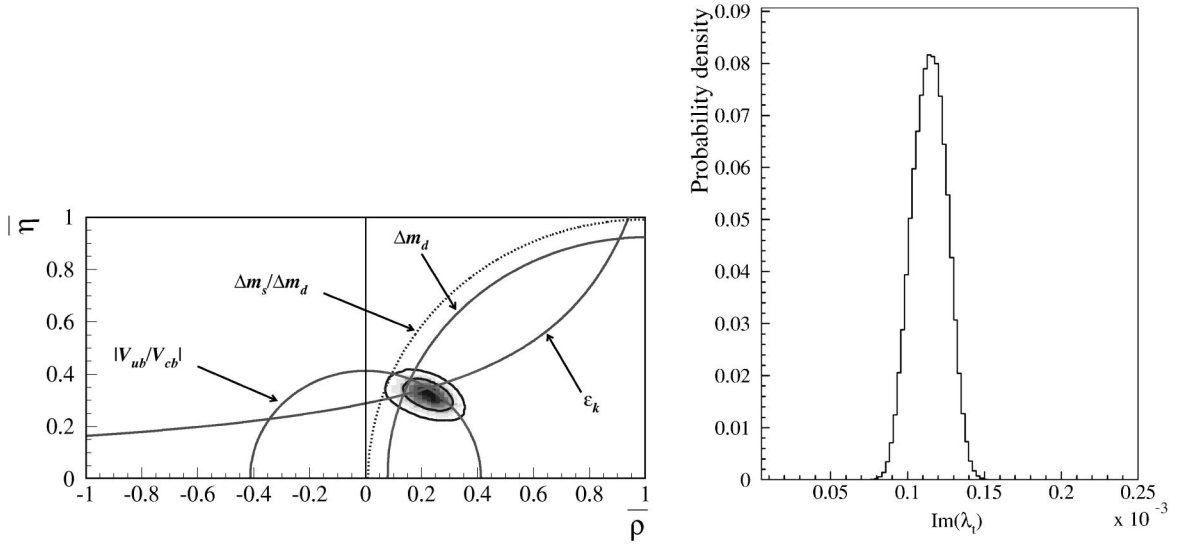


FIG. 4. Bounds on the Wolfenstein parameters $\bar{\eta} \equiv (1 - \lambda^2/2)$ and $\bar{\rho} \equiv (1 - \lambda^2/2)$ and distribution of $\text{Im} \lambda_1$, according to Parodi *et al.* for the input parameters in Table II.

correlated to the value of $\langle \alpha_s G G / \pi \rangle$ obtained in the fit of A_2 . We have verified that this affects the calculation of \hat{B}_K and the consequent determination of $\text{Im} \lambda_1$ in such a way to compensate numerically in ε'/ε the change of $\Omega_{\eta+\eta'}$. Waiting for a confident assessment of the NLO isospin violating effects in the $K \rightarrow \pi\pi$ amplitudes, we have used for $\Omega_{\eta+\eta'}$ the ‘LO’ value quoted in Table II.

The weak dependence on some poorly-known parameters is a welcome outcome of the correlation among hadronic matrix elements enforced in our semi-phenomenological approach by the fit of the $\Delta I = 1/2$ rule.

We have changed the central value of m_c from 1.4 GeV, the value we used in [17], to 1.3 GeV in order to make our estimate more homogeneous with others. This change affects the determination of the ranges of the model parameters, mainly increasing $\langle \bar{q}q \rangle$, via the fit of the CP conserving amplitudes. The central value of ε'/ε turns out to be affected below 10%.

While the χ QM approach to the hadronic matrix elements relevant in the computation of ε'/ε has many advantages over other techniques and has proved its value in the prediction of what has been then found in the experiments, it has a severe short-coming insofar as the matching scale has to be kept low, around 1 GeV and therefore the Wilson coefficients

have to be run down at scales that are at the limit of the applicability of the renormalization-group equations. Moreover, the matching itself suffers of ambiguities that have not been completely solved. For these reasons we have insisted all along that the approach is semi-phenomenological and that the above shortcomings are to be absorbed in the values of the input parameters on which the fit to the CP conserving amplitudes is based.

VI. OTHER ESTIMATES

Figure 7 summarizes the present status of theory versus experiment. In addition to our improved calculation (and an independent estimate similarly based on the χ QM), we have reported five estimates of ε'/ε published in the last year. Trieste’s, München’s and Roma’s ranges are updates of their respective older estimates, while the other estimates are altogether new.

The estimates reported come from the following approaches:

München’s [40]: In the München approach (phenomenological $1/N$) some of the matrix elements are obtained by fitting the $\Delta I = 1/2$ rule at $\mu = m_c = 1.3$ GeV. The relevant gluonic and electroweak penguin operators $\langle Q_6 \rangle$ and $\langle Q_8 \rangle_2$

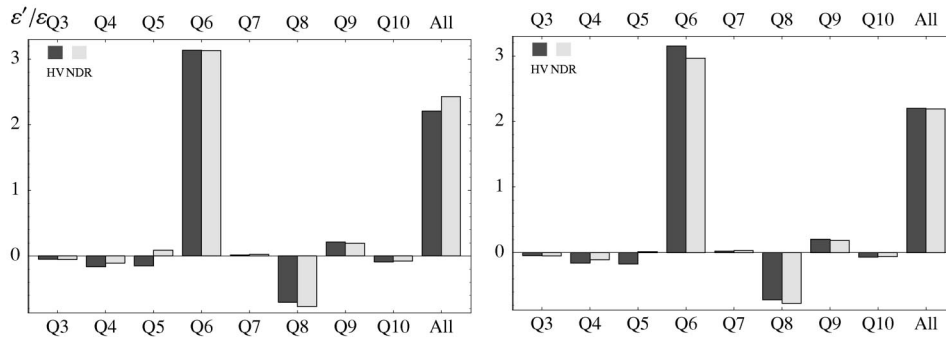


FIG. 5. Contribution to ε'/ε (in units of 10^{-3}) of each penguin operator in the HV and NDR γ_5 schemes. The figure on the left (right) corresponds to $\mu = 0.8$ (1.0) GeV.

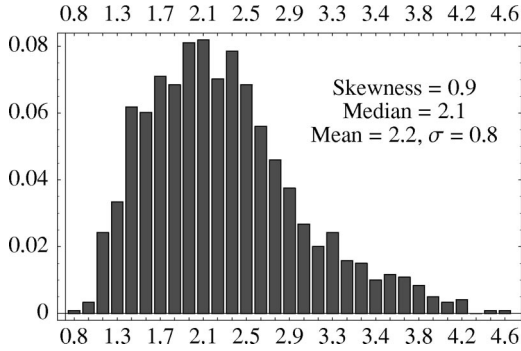


FIG. 6. Distribution of values of ε'/ε (in units of 10^{-3}). Normalized bins are plotted against the values of ε'/ε of each bin.

remain undetermined and are taken around their leading $1/N$ values (which implies a scheme dependent result). In Fig. 7 the HV (left) and NDR (right) results are shown. The darker range represents the result of Gaussian treatment of the input parameters compared to flat scanning (complete range).

Roma's [41]: Lattice cannot provide us at present with reliable calculations of the $I=0$ penguin operators relevant to ε'/ε as well as of the $I=0$ components of the hadronic matrix elements of the current-current operators (penguin contractions), which are relevant to the $\Delta I=1/2$ rule. This is due to large renormalization uncertainties, partly related to the breaking of chiral symmetry on the lattice. In this respect, very promising is the domain-wall fermion approach [42] which allows us to decouple the chiral symmetry from the continuum limit. On the other hand, present lattice calculations compute $K \rightarrow \pi$ matrix elements and use lowest order chiral perturbation theory to estimate the $K \rightarrow \pi\pi$ amplitude, which introduces additional (and potentially large) uncertainties. In the recent Roma re-evaluation of ε'/ε , B_6 is taken at the VSA result varied by a 100% error. The estimate quotes the values obtained in two γ_5 schemes (HV and NDR). The dark (light) ranges correspond to Gaussian (flat) scan of the input parameters.

Dortmund's [28]: In recent years the Dortmund group has revived and improved the approach of Bardeen, Buras and Gerard [43] based on the $1/N$ expansion. Chiral loops are regularized via a cutoff and the amplitudes are arranged in a p^{2n}/N expansion. A particular attention has been given to the matching procedure between the scale dependence of the chi-

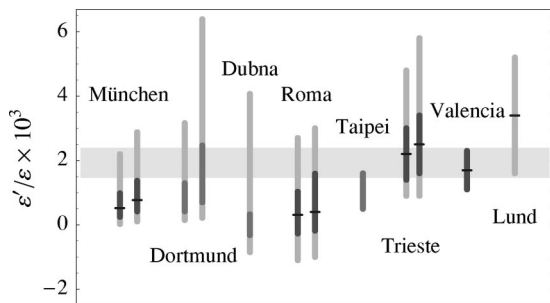


FIG. 7. Theory vs experiment in the year 2000. The gray band is the average experimental result. See the text for details on the various estimates.

ral loops and that arising from the short-distance analysis. The renormalization scheme dependence remains and it is included in the final uncertainty. The $\Delta I=1/2$ rule is reproduced, but the presence of the quadratic cutoff induces a matching scale instability (which is very large for B_K). The NLO corrections to $\langle Q_6 \rangle$ induce a substantial enhancement of the matrix element (right range in Fig. 7) compared to the leading order result (left). The dark range is drawn for central values of m_s , $\Omega_{\eta+\eta'}$, $\text{Im}\lambda_t$ and Λ_{QCD} .

Dubna's [22]: The hadronic matrix elements are computed in the Einstein NJL (ENJL) framework including chiral loops up to $O(p^6)$ and the effects of scalar, vector and axial-vector resonances. (B_K , and therefore $\text{Im}\lambda_t$, is taken from [15].) Chiral loops are regularized via the heat-kernel method, which leaves unsolved the problem of the renormalization scheme dependence. A phenomenological fit of the $\Delta I=1/2$ rule implies deviations up to a factor two on the calculated $\langle Q_6 \rangle$. The reduced (dark) range in Fig. 7 corresponds to taking the central values of the NLO chiral couplings and varying the short-distance parameters.

Taipei's [44]: Generalized factorization represents an attempt to parametrize the hadronic matrix elements in the framework of factorization without *a priori* assumptions [45]. Phenomenological parameters are introduced to account for non-factorizable effects. Experimental data are used in order to extract as much information as possible on the non-factorizable parameters. This approach has been applied to the $K \rightarrow \pi\pi$ amplitudes in Ref. [44]. The effective Wilson coefficients, which include the perturbative QCD running of the quark operators, are matched to the factorized matrix elements at the scale μ_F which is arbitrarily chosen in the perturbative regime. A residual scale dependence remains in the penguin matrix elements via the quark mass. The analysis shows that in order to reproduce the $\Delta I=1/2$ rule and ε'/ε sizable non-factorizable contributions are required both in the current-current and the penguin matrix elements. However, some assumptions on the phenomenological parameters and *ad hoc* subtractions of scheme-dependent terms in the Wilson coefficients make the numerical results questionable. In addition, the quoted error does not include any short-distance uncertainty.

Trieste's: The dark (light) ranges correspond to Gaussian (flat) scan of the input parameters. The bar on the left corresponds to the present estimate. That on the right is a new estimate [46], similarly based on the χ QM hadronic matrix elements, in which however ε'/ε is estimated in a novel way by including the explicit computation of ε in the ratio as opposed to the usual procedure of taking its value from the experiment. This approach has the advantage of being independent of the determination of the CKM parameters $\text{Im}\lambda_t$ and of showing more directly the dependence on the long-distance parameter \hat{B}_K as determined within the model. The difference (around 10%) between the two Trieste's estimates corresponds effectively to a larger value of $\text{Im}\lambda_t$, as determined from ε only, with respect to Eq. (4.8).

Valencia's [30]: The standard model estimate given by Pallante and Pich is obtained by applying the FSI correction factors obtained using a dispersive analysis in the manner of

Omnès-Mushkelishvili [47] to the leading (factorized) $1/N$ amplitudes. The detailed numerical outcome has been questioned on the basis of ambiguities related to the choice of the subtraction point at which the factorized amplitude is taken [48]. Large corrections may also be induced by unknown local terms which are unaccounted for by the dispersive resummation of the leading chiral logs. Nevertheless, the analysis of Ref. [30] confirms the crucial role of higher order chiral corrections for ε'/ε , even though FSI effects alone leave the problem of reproducing the $\Delta I=1/2$ selection rule open.

Lund's [49]: The $\Delta I=1/2$ rule and B_K have been studied in the NJL framework and $1/N$ expansion by Bijmens and Prades [29] showing an impressive scale stability when including vector and axial-vector resonances. A recent calculation of ε'/ε at the NLO in $1/N$ has been performed in Ref. [49]. The calculation is done in the chiral limit and it is eventually corrected by estimating the largest $SU(3)$ breaking effects. Particular attention is devoted to the matching between long- and short-distance components by use of the X -boson method [50,51]. The couplings of the X bosons are computed within the ENJL model which improves the high-energy behavior. The $\Delta I=1/2$ rule is reproduced and the computed amplitudes show a satisfactory renormalization scale and scheme stability. A sizable enhancement of the Q_6 matrix element is found which brings the central value of ε'/ε at the level of 3×10^{-3} .

Cutoff based approaches should also pay attention to higher-dimension operators which become relevant for matching scales below 2 GeV [52]. The calculations based on dimensional regularization may avoid the problem if phenomenological input is used in order to encode in the hadronic matrix elements the physics at all scales.

Other attempts to reproduce the measured ε'/ε using the linear σ -model, which include the effect of a scalar resonance with $m_\sigma \approx 900$ MeV, obtain the needed enhancement of $\langle Q_6 \rangle$ [53]. However, the CP conserving $I=0$ amplitude falls short the experimental value by a factor of two. With a lighter scalar, $m_\sigma \approx 600$ MeV the CP conserving $I=0$ amplitude is reproduced, but ε'/ε turns out more than one order of magnitude larger than currently measured [54].

VII. CONCLUSIONS

The present analysis updates our 1997 estimate $\text{Re } \varepsilon'/\varepsilon = 1.7_{-1.0}^{+1.4} \times 10^{-3}$ [17], which already pointed out the potential relevance of non-factorizable contributions and the importance of addressing both CP conserving and violating data for a reliable estimate of ε'/ε .

The increase in the central value is due to the update on the experimental inputs (mainly V_{ub}/V_{cb}). The uncertainty is reduced when using the Gaussian sampling, as opposed to the flat scan used in Ref. [17]. On the other hand the error obtained by flat scanning is larger due to the larger systematic uncertainty ($\pm 30\%$) used in the fit of the CP conserving amplitudes.

Among the corrections to the leading $1/N$ (factorized) result, FSI play a crucial role in the determination of the gluon penguin matrix elements. Recent dispersive analyses of $K \rightarrow \pi\pi$ amplitudes show how a (partial) resummation of FSI increases substantially the size of the $I=0$ amplitudes, while slightly affecting the $I=2$ components [30–32]. On the other hand, the precise size of the effect depends on boundary conditions of the factorized amplitudes which are not unambiguously known [48,55].

Finally, it is worth stressing that FSI by themselves do not account for the magnitude of the CP conserving decay amplitudes. In our approach a combination of non-factorizable soft-gluon effects [at $O(p^2)$] and FSI (at the NLO) makes possible to reproduce the $\Delta I=1/2$ selection rule. In turn, requiring the fit of the CP conserving $K \rightarrow \pi\pi$ decays allows for the determination of the “non-perturbative” parameters of the χ QM, which eventually leads to the detailed prediction of ε'/ε . Confidence in our final estimate of ε'/ε is based on the coherent picture of kaon physics which arises from the phenomenological determination of the model parameters and the self-contained calculation of all $\Delta S=1$ and 2 hadronic matrix elements.

ACKNOWLEDGMENT

We thank F. Parodi and A. Stocchi for their help in the determination of $\text{Im } \lambda_t$ and for Fig. 4.

-
- [1] G. C. Branco *et al.*, *CP Violation* (Oxford Science Publications, Oxford, 1999); A. I. Sanda and I. I. Bigi, *CP Violation* (Cambridge University Press, Cambridge, England, 1999).
 - [2] M. Gell-Mann and A. Pais, in *Proceedings of the Glasgow Conference on Nuclear and Meson Physics*, edited by E. H. Bellamy and R. G. Moorhouse (Pergamon, London, 1955), p. 342.
 - [3] L. H. Christenson *et al.*, *Phys. Rev. Lett.* **13**, 138 (1964).
 - [4] A. J. Buras *et al.*, *Nucl. Phys.* **B370**, 69 (1992); **B400**, 37 (1993); A. J. Buras, M. Jamin, and M. E. Lautenbacher, *ibid.* **B400**, 75 (1993); **B408**, 209 (1993); M. Ciuchini *et al.*, *ibid.* **B415**, 403 (1994).
 - [5] L. Wolfenstein, *Phys. Rev. Lett.* **13**, 562 (1964).
 - [6] B. Winstein and L. Wolfenstein, *Rev. Mod. Phys.* **65**, 1113 (1993).
 - [7] G. Buchalla, A. J. Buras, and M. E. Lautenbacher, *Rev. Mod. Phys.* **68**, 1125 (1996).
 - [8] S. Bertolini, J. Eeg, and M. Fabbrichesi, *Rev. Mod. Phys.* **72**, 65 (2000).
 - [9] *The Second DAPHNE Physics Handbook*, edited by L. Maiani, G. Pancheri, and N. Paver (SIS, INFN-LNF, Frascati, Italy, 1995).
 - [10] NA31 Collaboration, G. D. Barr *et al.*, *Phys. Lett. B* **317**, 233 (1993).
 - [11] E731 Collaboration, L. K. Gibbons *et al.*, *Phys. Rev. D* **55**, 6625 (1997).
 - [12] KTeV Collaboration, A. Alavi-Harati *et al.*, *Phys. Rev. Lett.* **83**, 22 (1999).
 - [13] NA48 Collaboration, V. Fanti *et al.*, *Phys. Lett. B* **465**, 335 (1999).

- [14] NA48 Collaboration, A. Ceccucci, <http://www.cern.ch/NA48/Welcome.html>.
- [15] A. J. Buras, M. Jamin, and M. E. Lautenbacher, Nucl. Phys. **B370**, 209 (1993).
- [16] M. Ciuchini, Nucl. Phys. B (Proc. Suppl.) **59**, 149 (1997).
- [17] S. Bertolini *et al.*, Nucl. Phys. **B514**, 63 (1998); **B514**, 93 (1998).
- [18] K. Nishijima, Nuovo Cimento **11**, 698 (1959); F. Gursey, *ibid.* **16**, 23 (1960); Ann. Phys. (N.Y.) **12**, 91 (1961); J. A. Cronin, Phys. Rev. **161**, 1483 (1967); S. Weinberg, Physica A **96**, 327 (1979); A. Manohar and H. Georgi, Nucl. Phys. **B234**, 189 (1984); A. Manohar and G. Moore, *ibid.* **B243**, 55 (1984); D. Espriu *et al.*, *ibid.* **B345**, 22 (1990).
- [19] Y. Nambu and G. Jóna-Lasinio, Phys. Rev. **122**, 345 (1961); J. Bijnens, Phys. Rep. **265**, 369 (1996).
- [20] A. Pich and E. de Rafael, Nucl. Phys. **B358**, 311 (1991).
- [21] E. Chell and M. G. Olsson, Phys. Rev. D **48**, 4076 (1993).
- [22] A. A. Bel'kov *et al.*, hep-ph/9907335.
- [23] J. Bijnens, Int. J. Mod. Phys. A **8**, 3045 (1993).
- [24] T. Inami and C. S. Lim, Prog. Theor. Phys. **65**, 297 (1981).
- [25] S. Peris and E. de Rafael, Phys. Lett. B **490**, 213 (2000).
- [26] L. Lellouch, hep-lat/0011088.
- [27] JLQCD Collaboration, S. Aoki *et al.*, Phys. Rev. Lett. **80**, 5271 (1998).
- [28] T. Hambye *et al.*, Nucl. Phys. **B564**, 391 (2000); hep-ph/0001088.
- [29] J. Bijnens and J. Prades, J. High Energy Phys. **01**, 023 (1999).
- [30] E. Pallante and A. Pich, Phys. Rev. Lett. **84**, 2568 (2000); Nucl. Phys. **B592**, 294 (2000).
- [31] J. F. Donoghue and E. Golowich, Phys. Lett. B **478**, 172 (2000).
- [32] E. A. Paschos, hep-ph/9912230.
- [33] M. Knecht, S. Peris, and E. de Rafael, Phys. Lett. B **457**, 227 (1999).
- [34] A. J. Buras, M. Jamin, and P. H. Weisz, Nucl. Phys. **B347**, 491 (1990); S. Herrlich and U. Nierste, *ibid.* **B419**, 292 (1994); Phys. Rev. D **52**, 6505 (1995); Nucl. Phys. **B476**, 27 (1996).
- [35] P. Paganini *et al.*, Phys. Scr. **58**, 556 (1998); F. Parodi, P. Roudeau, and A. Stocchi, Nuovo Cimento A **112**, 833 (1999).
- [36] G. Ecker *et al.*, Phys. Lett. B **467**, 88 (2000).
- [37] S. Gardner and G. Valencia, Phys. Lett. B **466**, 355 (1999); Phys. Rev. D **62**, 094024 (2000).
- [38] K. Maltman and C. Wolfe, Phys. Lett. B **482**, 77 (2000); C. Wolfe and K. Maltman, Phys. Rev. D **63**, 014008 (2001).
- [39] V. Cirigliano, J. F. Donoghue, and E. Golowich, Phys. Lett. B **450**, 241 (1999); Phys. Rev. D **61**, 093001 (2000); **61**, 093002 (2000); Eur. Phys. J. C **18**, 83 (2000).
- [40] S. Bosch *et al.*, Nucl. Phys. **B565**, 3 (2000).
- [41] M. Ciuchini *et al.*, Nucl. Phys. **B573**, 201 (2000).
- [42] D. Kaplan, Phys. Lett. B **288**, 342 (1992); A. Soni, Proceedings of the \mathcal{B}_{CP} Conference, Taipei, Taiwan, 1999.
- [43] W. A. Bardeen, A. J. Buras, and J. M. Gerard, Nucl. Phys. **B293**, 787 (1987).
- [44] H.-Y. Cheng, Chin. J. Phys. (Taipei) **38**, 1044 (2000).
- [45] M. Neubert and B. Stech, hep-ph/9705292.
- [46] M. Fabbrichesi, Phys. Rev. D **62**, 097902 (2000).
- [47] N. I. Mushkelishvili, *Singular Integral Equations* (Noordhoff, Gronigen, 1953), p. 204; R. Omnès, Nuovo Cimento **8**, 316 (1958).
- [48] A. J. Buras *et al.*, Phys. Lett. B **480**, 80 (2000).
- [49] J. Bijnens and J. Prades, J. High Energy Phys. **06**, 035 (2000).
- [50] W. A. Bardeen, J. Bijnens, and J.-M. Gérard, Phys. Rev. Lett. **62**, 1343 (1989); J. Bijnens, J.-M. Gérard, and G. Klein, Phys. Lett. B **257**, 191 (1991); J. P. Fatelo and J.-M. Gérard, *ibid.* **347**, 136 (1995).
- [51] J. Bijnens and J. Prades, Phys. Lett. B **342**, 331 (1995); Nucl. Phys. **B444**, 523 (1995); J. High Energy Phys. **01**, 023 (1999); **01**, 002 (2000).
- [52] V. Cirigliano, J. F. Donoghue, and E. Golowich, J. High Energy Phys. **10**, 048 (2000).
- [53] Y. Y. Keum, U. Nierste, and A. I. S. Sanda, Phys. Lett. B **457**, 157 (1999); M. Harada *et al.*, Phys. Rev. D **62**, 014002 (2000).
- [54] J. C. R. Bloch *et al.*, Phys. Rev. C **62**, 025206 (2000).
- [55] M. Suzuki, hep-ph/0001170.